INTERNATIONAL JOURNAL OF
NUMERICAL ANALYSIS AND MODELING
Volume 13, Number 5, Pages 739–752

A CONSERVATIVE ENFORCING POSITIVITY-PRESERVING ALGORITHM FOR DIFFUSION SCHEME ON GENERAL MESHES

FUJUN CAO, YANZHONG YAO, YUNLONG YU, AND GUANGWEI YUAN*

Abstract. For a class of diffusion schemes not satisfying the property of positivity-preserving, we propose an enforcing positivity algorithm. It is locally conservative and easy to be implemented in existing codes. Moreover, this algorithm can be performed on both structured and unstructured meshes. Numerical experiments demonstrate that in terms of L_2 error and conservation this algorithm is much better than the trick of directly enforcing the negative values to zero (ENZ), which has been used in applications, meanwhile, in terms of L_∞ error it is approximate to ENZ and CEPA repairing algorithms.

Key words. positivity correction, conservation, nonlinear diffusion equation, general mesh.

1. Introduction

Diffusion process appears in many physical problems, such as the subsurface flows, radioactive material transport and inertia confinement fusion. While numerically simulating those problems, in order to obtain reliable numerical solution, it is necessary for the numerical methods to preserve some basic properties of diffusion equation such as the conservation and the maximum principle. Unfortunately, most of the discrete schemes for diffusion equations can not satisfy the discrete maximum principle(DMP) on distorted meshes, including some well-known diffusion schemes, such as the Kershaw scheme presented in [4], the MDHW scheme proposed in [10], the Nine-Point scheme (NPS) in [6], the multi-point flux approximation (MPFA) in [1], and the mimetic finite difference (MFD) methods in [7, 8]. A scheme not satisfying the DMP may produce negative numerical solution for diffusion equation with nonnegative initial value and sources term.

As it was pointed out in [14], the positivity of solutions is very important for numerical robustness. For some nonlinear diffusion problems, diffusion coefficients have no definition for negative solutions. If the numerical solutions are negative values in the process of computation, the computation procedure will break down. In order to prevent the computation procedure from interrupting, one common way is to modify the negative values by using certain repair techniques, and then the positivity-preserving can be achieved. Another way is to design positivity-preserving schemes, such as those in [2], [11], [12], [16], [21] and [22]. But, as we know, all of them with the accuracy being higher than first order are nonlinear schemes even if the diffusion equation is linear, so the computational costs will increase unavoidably.

This paper will focus on the first way of mending the "negative" cells, i.e., the numerical solutions of finite volume scheme on those cells are negative. The simplest repair technique for a posteriori correction of the discrete solution is just to

Received by the editors March 22, 2016 and, in revised form, July 17, 2016.
2000 *Mathematics Subject Classification.* 35R35, 49J40, 60G40.
*Corresponding author. This work was supported by the National Nature Science Foundation of China (11571048, 11571047, 11671049).

set negative values to be zero (or a small positive number), which is easy to be implemented in existing codes but it destroys the conservation. Some improved strategies are proposed in recent years. In [9] a repair technique is proposed which enforces the linear finite element solution of elliptic equations on 2D triangular meshes to satisfy the discrete maximum principle and keep the total energy conservation. In [17] a global repair technique is devised for diamond finite volume schemes, which also keeps total energy conservation. In [5] a nonlinear constrained finite element method satisfying the discrete maximum principle to anisotropic diffusion problems is proposed, which is a positivity-preserving correction scheme. All of these repair algorithms do not maintain local conservation, i.e., they don't give consistent discrete flux on cell-edges between the neighboring cells.

In [20] a method of enforcing positivity with local conservation for nine-point schemes of nonlinear diffusion equations is developed, which allows the new solution to preserve positivity as well as local conservation at each nonlinear iteration step in solving nonlinear diffusion problems. However, this method may lead to the increase of the number of nonlinear iteration, and then computational efficiency decreases.

In this paper we develop an efficient method of enforcing negative values to zero with local conservation for nonlinear diffusion equations on both structure and unstructured meshes. It allows the new solution to preserve positivity as well as local conservation at each nonlinear iteration step .

This paper is organized as follows. In Section 2, we introduce a finite volume scheme on polygonal meshes for nonlinear diffusion equation. In Section 3, the conservative enforcing positivity-preserving algorithm is discussed. In Section 4, we give some numerical examples to verify the accuracy and conservation for our algorithm. The conclusion is summarized in Section 5.

2. The finite volume scheme on general meshes

Consider the nonlinear diffusion problem

$$\frac{\partial u}{\partial t} - \nabla \cdot (\kappa(X,t,u)\nabla u) = f(X,t), \quad X \in \Omega, \quad t \in (0,T], \tag{1}$$

$$u(X,0) = \phi(X), \quad X \in \Omega, \tag{2}$$

$$u(X,t) = \psi(X,t), \quad X \in \partial\Omega, t \in [0,T], \tag{3}$$

where $u = u(X,t)$ is a function to be solved, Ω is a polygonal domain in R^2, $X = (x,y) \in \Omega$, κ is a positive diffusion coefficient which may depend on u and could be discontinuous on Ω, and f is a given source function. The boundary conditions can also be Neumann or Robin types.

Divide Ω into polygonal meshes (see Fig. 1), in which a polygonal cell and its center are denoted by K or L. The cell edge is denoted by σ. If the σ is a common edge of cell K and L, and its vertices are A and B, then we denote $\sigma = K|L = BA$. Let $\mathcal{T}$ be the set of all cells, and $\mathcal{C}$ is the set of all cell-edges, and $\mathcal{C}_K$ is the set of all cell-edges of cell K. The length of σ is denoted by $|\sigma|$, and the area of cell K is denoted by S_K. The distance from the center of the cell K or L to the edge σ is denoted by $d_{K,\sigma}$ or $d_{L,\sigma}$ respectively. As usual we introduce a time step $\Delta t > 0$ and the time levels $t^n = n\Delta t$ with $n = 0, 1, \ldots, N$, and $t^N = T$.

By integrating (1) over the cell K and using the Green's formula, we can obtain

$$\int_K \frac{\partial u}{\partial t} dX + \sum_{\sigma \in \mathcal{C}_K} \mathcal{F}_{K,\sigma} = \int_K f(X,t) dX, \tag{4}$$

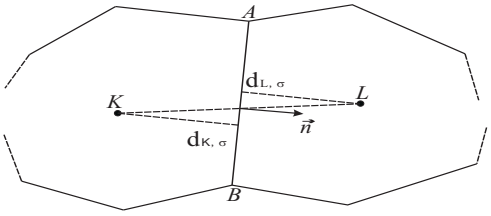

Figure 1: The polygonal meshes.

where $\mathcal{F}_{K,\sigma}$ is the normal flux on the edge σ, and is defined by

$$\mathcal{F}_{K,\sigma} = -\int_{\sigma} \kappa(X,t,u)\nabla u(X,t)\cdot \vec{n}_{K,\sigma} dl, \tag{5}$$

where $\vec{n}_{K,\sigma}$ is the outward unit normal on the edge σ of the cell K. Adopting the procedure in [6, 15], we can obtain

$$\mathcal{F}_{K,\sigma} = \tau_\sigma(u(K,t) - u(L,t) - D_\sigma(u(B,t) - u(A,t))) + O(h^2), \tag{6}$$

where $\tau_\sigma = \frac{\tau_{K,\sigma}\tau_{L,\sigma}}{\tau_{K,\sigma}+\tau_{L,\sigma}}$, and $\tau_{K,\sigma} = |\sigma|\frac{\kappa_K}{d_{K,\sigma}}$, $\tau_{L,\sigma} = |\sigma|\frac{\kappa_L}{d_{L,\sigma}}$, $h = \max\limits_{K\in\mathcal{T}} \mathrm{diam}K$ and $\kappa_K = \kappa(K,t)$ and $\kappa_L = \kappa(L,t)$ are diffusion coefficients on cells K and L respectively, and $D_\sigma = \frac{(\overrightarrow{KL},\overrightarrow{BA})}{|\sigma|^2}$, in which $(\overrightarrow{KL},\overrightarrow{BA})$ denotes the inner product for the vectors $\overrightarrow{KL}$ and $\overrightarrow{BA}$.

The discrete unknowns defined at cell-centers K, L and cell-vertices A,B are denoted by u_K, u_L and u_A,u_B , respectively. Then the implicit scheme of the problem (2.1)-(2.3) is given as follows

$$\frac{u_K^{n+1} - u_K^n}{\Delta t} + \frac{1}{S_K}\sum_{\sigma\in\mathcal{C}_K} \mathrm{F}_{K,\sigma}^{n+1} = f_K^{n+1}, \quad K\in\mathcal{T}, \tag{7}$$

where

$$\mathrm{F}_{K,\sigma}^{n+1} = \tau_\sigma^{n+1}((u_K^{n+1} - u_L^{n+1}) - D_\sigma(u_B^{n+1} - u_A^{n+1})), \quad \sigma\in\mathcal{C}_K\cap\mathcal{C}_L = BA = K|L, \tag{8}$$

$$\mathrm{F}_{K,\sigma}^{n+1} = \tau_{K,\sigma}^{n+1}((u_K^{n+1} - \psi_X^{n+1}) - D_{K,\sigma}(\psi_B^{n+1} - \psi_A^{n+1})), \quad \sigma\in\mathcal{C}_K\cap\partial\Omega = AB, \tag{9}$$

and $D_{K,\sigma} = \frac{(\overrightarrow{KX},\overrightarrow{BA})}{|\sigma|^2}$, $f_K^{n+1} = f(K,t^{n+1})$, $\psi_B^{n+1} = \psi(B,t^{n+1})$, $\psi_A^{n+1} = \psi(A,t^{n+1})$, and $\psi_X^{n+1} = \psi(X,t^{n+1})$, where X is the midpoint of the boundary edge.

In (7), in addition to cell-centered unknowns, there are some cell-vertex unknowns, such as u_A^{n+1} and u_B^{n+1}. Usually, in order to reduce computational cost the cell-vertex values are taken as intermediate unknowns, i.e., they are replaced by certain combinations of neighboring cell-centered values as follows

$$u_A^{n+1} = \frac{1}{\sum_{I\in\mathcal{B}(A)}\omega_I^{n+1}}\sum_{I\in\mathcal{B}(A)}\omega_I^{n+1}u_I^{n+1}, \tag{10}$$

where $\mathcal{B}(A)$ is the set of these cells with A as a vertex. There are some simple methods to compute the weighted factors ω_I^{n+1}, such as the arithmetic average weighted mode, i.e., $\omega_I^{n+1} = \frac{1}{N_A}$, and the inverse distance weighted mode, i.e., $\omega_I^{n+1} = \frac{\kappa_I^{n+1}}{d_{I,A}}$, where N_A is the number of cells in $\mathcal{B}(A)$ and $d_{I,A}$ is the distance between the center of cell I and the vertex A. These two modes have acceptable accuracy on smooth and uniform meshes, but when the meshes are highly distorted,

the accuracy will be very low. In recent years some works have been devoted to improve the accuracy of computing the cell-vertex values on distorted grids, such as [13], [15], [18] and [19]. In our numerical experiments, the weighted interpolation formula in [19] will be used.

3. Conservative positivity-preserving algorithm on general mesh

We use the Picard iteration method to linearize the nonlinear system (7) and the linear system is solved by the Bi-Conjugate Gradient Stabilized (BiCGStab) method. For the sake of simplicity, we omit the superscript $n+1$ of the value at the present time level, i.e., u_K represents u_K^{n+1}. The superscript n of u_K^n at the previous time level is preserved to avoid confusion. Let s be the nonlinear iteration index, and the iteration formulae are as follows,

$$\frac{u_K^{(s+1)}-u_K^n}{\Delta t}+\frac{1}{S_K}\sum_{\sigma\in\mathcal{C}_K}\mathrm{F}_{K,\sigma}^{(s+1)}=f_K^{n+1},\quad K\in\mathcal{T}, \tag{11}$$

$$\mathrm{F}_{K,\sigma}^{(s+1)}=\tau_\sigma^{(s)}((u_K^{(s+1)}-u_L^{(s+1)})-D_\sigma(u_B^{(s)}-u_A^{(s)})). \tag{12}$$

Note that the diffusion coefficient above is linearized by taking the values at the previous nonlinear iteration step. $(u_B^{n+1}-u_A^{n+1})$ is also set to be the values at the previous nonlinear iteration step so that it is convenient to solve the linear system.

Suppose that we get the solution values $u_K^{(s+1)}$ at the $(s+1)$-th iteration step. Because the finite volume scheme (7) is not a positivity-preserving scheme, so the numerical solutions in some cells may be negative even if the initial values and source items are nonnegative. Now we devise a conservative enforcing positivity-preserving algorithm to fix the values for these cells.

We divide the set of all grid-cells $\mathcal{T}$ into three subsets, as shown in Fig. 2, $\mathcal{T}=\mathbb{N}\cup\mathbb{P}^c\cup\mathbb{P}^+$, where $\mathbb{N}$ is the subset of those grid-cells on which $u_K^{(s+1)}<0$, $\mathbb{P}^+$ is the subset of those grid-cells on which $u_K^{(s+1)}\geq 0$, $\mathbb{P}^c$ is the subset of those grid-cells which have been repaired by using the enforcing positivity-preserving algorithm, and initially $\mathbb{P}^c$ is a null set.

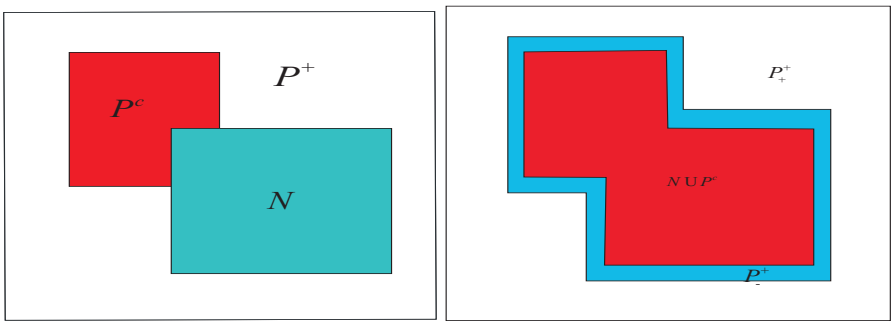

Figure 2: Classification of cells.

At the $(s+1)$-th nonlinear iteration step, if $\mathbb{N}$ is non-empty, i.e., there are negative solution values in some cells, and we will repair them according to the following procedure.

3.1. Enforcing positivity for cells in $\mathbb{N}$. The set $\mathbb{P}^c \cup \mathbb{N}$ is composed of the union of disjoint connected subsets RN_m, i.e., $\mathbb{P}^c \cup \mathbb{N} = \cup_{m=1}^{M} RN_m$, where M is the number of these subsets. The repair procedure is preformed for each RN_m.

Define the set $\mathbb{S}_m^0 = \{\sigma : \sigma \in \mathcal{C}_K \cap \mathcal{C}_{K^0}, K \in RN_m, K^0 \in \mathbb{P}^+\}$, whose elements are the boundary edges of m-th subset RN_m .

If $u_K^{(s+1)} < 0$, $K \in RN_m$, its value is enforced to be zero and denoted as $\tilde{u}_K^{(s+1)} = 0$. In order to keep local conservation, the fluxes across its surrounding edges are also should be revised, we use $\tilde{F}_{K,\sigma}^{(s+1)}$ to denote the modified fluxes, and require that the revised values and the fluxes satisfy the following equation

$$\frac{\tilde{u}_K^{(s+1)} - u_K^n}{\Delta t} + \frac{1}{S_K} \sum_{\sigma \in \mathcal{C}_K} \tilde{F}_{K,\sigma}^{(s+1)} = f_K^{n+1}, \qquad K \in RN_m. \tag{13}$$

Summating above equation over $K \in RN_m$, and according to the local flux conservation condition $\tilde{F}_{K,\sigma} = -\tilde{F}_{L,\sigma}, \forall \sigma = K|L$, we can get

$$\frac{1}{\Delta t} \sum_{K \in RN_m} (\tilde{u}_K^{(s+1)} - u_K^n) S_K + \sum_{\sigma \in \mathbb{S}_m^0} \tilde{F}_{K,\sigma}^{(s+1)} = \sum_{K \in RN_m} f_K^{n+1} S_K. \tag{14}$$

Similarly, the following formula can be obtained from (11) by summating it over $K \in RN_m$

$$\frac{1}{\Delta t} \sum_{K \in RN_m} (u_K^{(s+1)} - u_K^n) S_K + \sum_{\sigma \in \mathbb{S}_m^0} F_{K,\sigma}^{(s+1)} = \sum_{K \in RN_m} f_K^{n+1} S_K. \tag{15}$$

Subtracting (15) from (14), we can get the relationship between the revised fluxes and the original fluxes as follows

$$\sum_{\sigma \in \mathbb{S}_m^0} (\tilde{F}_{K,\sigma}^{(s+1)} - F_{K,\sigma}^{(s+1)}) = -\frac{\Delta E}{\Delta t}, \tag{16}$$

where

$$\Delta E = \sum_{K \in RN_m} (\tilde{u}_K^{(s+1)} - u_K^{(s+1)}) S_K. \tag{17}$$

A natural way for the choice of the revised fluxes is

$$\tilde{F}_{K,\sigma}^{(s+1)} = F_{K,\sigma}^{(s+1)} - w_\sigma \frac{\Delta E}{\Delta t}, \qquad \sigma \in \mathbb{S}_m^0, \tag{18}$$

where the w_σ is

$$w_\sigma = \frac{|\sigma|}{\sum_{\sigma^* \in \mathbb{S}_m^0} |\sigma^*|}. \tag{19}$$

In fact, more choice can be designed for the coefficient w_σ , such as $w_\sigma = \frac{1}{N_\sigma}$, where N_σ is the number of elements in the set $\mathbb{S}_m^0$.

3.2. Updating the cells in $\mathbb{P}^+$ for conservation. The physical conservation requires that the fluxes on the common edges of adjacent cells satisfy the following relationship, $F_{K,\sigma} = -F_{L,\sigma}, \sigma = \partial K \bigcap \partial L$. So we need to revise the fluxes of cell in $\mathbb{P}^+$ to keep the local conservation.

Firstly, we divide the set $\mathbb{P}^+$ into two subsets, $\mathbb{P}^+ = \mathbb{P}_+^+ \cup \mathbb{P}_-^+$. $\mathbb{P}_+^+ = \{K : K \in \mathbb{P}^+, \forall K_i \in \pi_K, K_i \in \mathbb{P}^+\}$, where π_K is the set of cells which have common edge with cell K. $\mathbb{P}_-^+ = \{K : K \in \mathbb{P}^+, \exists K_i \in \pi_K, K_i \notin \mathbb{P}^+\}$.

For any $K \in \mathbb{P}_+^+$, we keep its values and flux on edge not to be repaired, i.e.,

$$\tilde{u}_K^{(s+1)} = u_K^{(s+1)}, \quad \tilde{F}_{K,\sigma}^{(s+1)} = F_{K,\sigma}^{(s+1)}, \quad \forall \sigma \in \mathcal{C}_K. \tag{20}$$

For $\forall K \in \mathbb{P}_-^+$, $\sigma \in \mathcal{C}_K$, if $\sigma \notin \mathbb{S}_m^0$ then

$$\tilde{F}_{K,\sigma}^{(s+1)} = F_{K,\sigma}^{(s+1)}, \tag{21}$$

else if $\sigma \in \mathbb{S}_m^0$, then

$$\tilde{F}_{K,\sigma}^{(s+1)} = F_{K,\sigma}^{(s+1)} + w_\sigma \frac{\Delta E}{\Delta t}. \tag{22}$$

Next, we use the revised fluxes to renew the values on the cell K

$$\frac{\tilde{u}_K^{(s+1)} - u_K^n}{\Delta t} + \frac{1}{S_K} \sum_{\sigma \in \mathcal{C}_K} \tilde{F}_{K,\sigma}^{(s+1)} = f_K^{n+1}, \qquad K \in \mathbb{P}_-^+. \tag{23}$$

From (21)-(23), the revised values satisfy the following equation

$$\frac{\tilde{u}_K^{(s+1)} - u_K^n}{\Delta t} + \frac{1}{S_K} \sum_{\sigma \in \mathcal{C}_K} F_{K,\sigma}^{(s+1)} + \frac{1}{S_K} \sum_{\sigma \in \mathcal{C}_K \bigcap \mathbb{S}_m^0} w_\sigma \frac{\Delta E}{\Delta t} = f_K^{n+1}, \qquad K \in \mathbb{P}_-^+. \tag{24}$$

Subtract the formula (11) from (24) and multiply Δt, we can get

$$\tilde{u}_K^{(s+1)} - u_K^{(s+1)} + \frac{1}{S_K} \sum_{\sigma \in \mathcal{C}_K \bigcap \mathbb{S}_m^0} w_\sigma \Delta E = 0, \tag{25}$$

i.e.,

$$\tilde{u}_K^{(s+1)} = u_K^{(s+1)} - \frac{1}{S_K} \sum_{\sigma \in \mathcal{C}_K \bigcap \mathbb{S}_m^0} w_\sigma \Delta E. \tag{26}$$

Obviously, the calculation of $\tilde{u}_{K,\sigma}^{(s+1)}$ here is explicit. For the cell K, if only one flux (e.g., that across the edge σ) is changed, then we can set

$$\tilde{u}_K^{(s+1)} = u_K^{(s+1)} - w_\sigma \frac{\Delta E}{S_K}. \tag{27}$$

We call this algorithm as the General Conservative Enforcing Negative values to Zero, which is abbreviated to GCENZ.

3.3. Accuracy analysis for GCENZ. Now we consider the accuracy of the repaired solution given by the conservative repair algorithm GCENZ. For a cell K with negative value at time $t = t^{n+1}$, the error of the original (unrepaired) discrete solution is

$$e(K,t) = |u_K^{(s+1)} - u(K,t)|, \tag{28}$$

and the error of the repaired discrete solution is

$$\tilde{e}(K,t) = |\tilde{u}_K^{(s+1)} - u(K,t)|, \tag{29}$$

where the $u(K,t)$ is the exact solution at (K,t). Obviously, since

$$u_K^{(s+1)} < 0, \quad u(K,t) \geq 0, \quad \tilde{u}_K^{(s+1)} = 0 \tag{30}$$

we can get

$$e(K,t) > u(K,t) = \tilde{e}(K,t), \tag{31}$$

so the accuracy of numerical solution by GCENZ algorithm is definitely improved for the negative cells.

For a cell L with positive value which is updated from the conservation requirement, the updated value is given by (27). Suppose the discrete solution $u_X^{(s+1)}$ is the p-th order approximation to $u(X,t)$, i.e.,

$$u_X^{(s+1)} = u(X,t) + O(h^p), \tag{32}$$

and the repaired solution satisfies

$$\tilde{u}_K^{(s+1)} - u_K^{(s+1)} = O(h^{p+1}), \tag{33}$$

moreover,the number of negative cells account for a small portion of total cells's

$$N_{RN_m} = O(1/h), \tag{34}$$

where N_{RN_m} denotes the number of elements in the set RN_m, then in terms of (17) and (27) we have

$$\tilde{u}_L^{(s+1)} = u(L,t) + O(h^p). \tag{35}$$

3.4. Procedure of GCENZ. The GCENZ procedure algorithm is given as follows:

(1) Solve the $(s+1)$-th iteration step to obtain the cell-centered values $u_K^{(s+1)}$ and cell-edge flux of cell K, $\{F_{K,\sigma}^{(s+1)} | \sigma \in \mathcal{C}_K\}$.
(2) All the cells are divided into three sets $\mathbb{N}, \mathbb{P}^+, \mathbb{P}^c$, where $\mathbb{N}$ is the set of negative cells, $\mathbb{N} = \{K : u_K < 0\}$, $\mathbb{P}^c$ is the set of cells whose values are initially negative in $(s+1)$-th step and have been repaired, $\mathbb{P}^+$ is the set of positive cells.
(3) If all cell-centered values are nonnegative, i.e., $N = \emptyset$, then goto 7, else goto the next step.
(4) Classify all the cells in $\mathbb{P}^c \cup \mathbb{N}$ into connected subsets $\{RN_m, m = 1, \cdots, M\}$ according to their connectivity.
(5) Preform the conservative repair method for each subset RN_m according to the algorithm presented in subsections (3.1)-(3.2).
(6) Goto 2.
(7) Goto 1 and execute the nonlinear iteration step until the convergence criterion holds.

4. Numerical experiments

In this section, we give some numerical examples on distorted grids to verify the efficiency and the accuracy of GCENZ method. The comparison of GCENZ with other repair algorithms is presented by giving L_2, L_∞ and conservation errors.

The L_∞ and L_2 norms of errors are defined as follows:

$$e_{L_\infty} = \max_{K \in \mathcal{T}} \left| u(K,T) - u_K^N \right|, \tag{36}$$

$$e_{L_2} = \left(\sum_{K \in \mathcal{T}} (u(K,T) - u_K^N)^2 S_K \right)^{1/2}, \tag{37}$$

where $u(K,T)$ is the reference solution defined in the center of the grids at the time T, which maybe the exact solution or the numerical solution on the refined orthogonal grids. u_K^N is the numerical solution at the time $T = N\Delta t$.

The conservation error of the numerical solution is defined as follows:

$$e_{dcon} = \left| \sum_{K \in \mathcal{T}} u_K^N S_K - \sum_{K \in \mathcal{T}} u_K^0 S_K + \sum_{n=1}^{N} \left(\sum_{\sigma \in \partial\Omega} F_{K,\sigma}^n \right) \triangle t - \sum_{n=1}^{N} \left(\sum_{K \in \mathcal{T}} f_K^n S_K \right) \triangle t \right|. \tag{38}$$

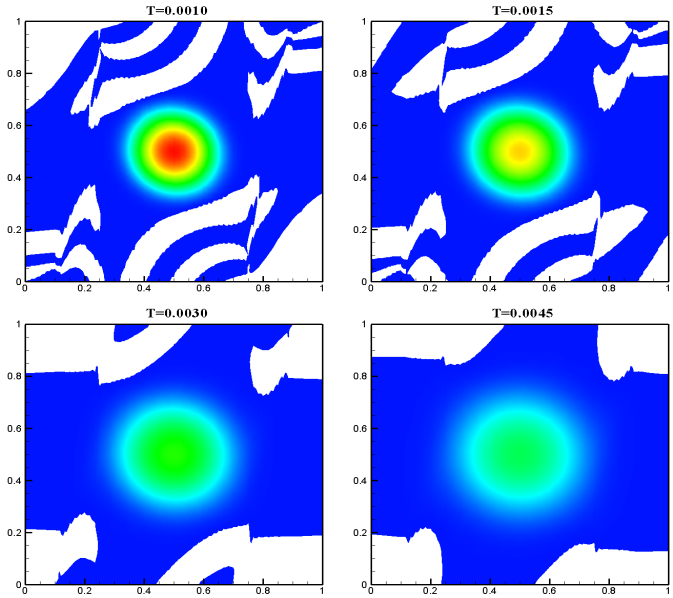

Figure 3: The solutions at $T = 0.001, 0.0015, 0, 003, 0.0045$ on Kershaw mesh.

In the following examples, the computational domain is $\Omega = (0,1) \times (0,1)$, and the nonlinear convergence criterion is

$$\max_{K \in \mathcal{T}} |u_K^{(s+1)} - u_K^{(s)}| < \varepsilon. \tag{39}$$

Example 1 First, we consider the following linear model with Neumann boundary condition:

(40)
$$\begin{cases} \frac{\partial u}{\partial t} - \operatorname{div}(\nabla u) = 0, & (x,y,t) \in \Omega \times (0,T], \\ u(x,y,0) = 10 \exp\left(\frac{a^2(x-c)^2+b^2(y-c)^2}{a^2(x-c)^2+b^2(y-c)^2-a^2b^2}\right), & a^2(x-c)^2 + b^2(y-c)^2 < a^2b^2, \\ u(x,y,0) = 0, & a^2(x-c)^2 + b^2(y-c)^2 \geq a^2b^2, \\ \frac{\partial}{\partial \vec{n}} u(x,y,t) = 0, & (x,y) \in \partial\Omega, t \in (0,T], \end{cases}$$

where $\vec{n}$ is the unit normal vector outward on $\partial\Omega$. We choose $a^2 = b^2 = 0.01$,$c = 0.5$. The exact solution is not known for this linear problem, so we solve it on 200×200 rectangular grids, and then take these numerical solutions as the reference solutions. We choose $\Delta t = 10^{-6}$, $T = 0.01$, and the convergence criterion is $\varepsilon = 10^{-6}$.

First, we test this problem on Kershaw mesh and the number of cell is 50×50. The numerical solutions using the scheme (7) are shown in Fig. 3. It displays the numerical solution at different time. The blank part in the figures represents negative cells.

For this example, we use GCENZ algorithm to repair the numerical solution, and compare the results from this algorithm with those from the ENZ and CEPA repair algorithms. ENZ is the directly enforcing the negative values to zero algorithm, which is a traditional repair way, but it is not a conservation method and the conservation error is ascending with the time increasing. CEPA is the repair algorithm presented in [20]. Fig. 4 presents the conservation errors in terms of

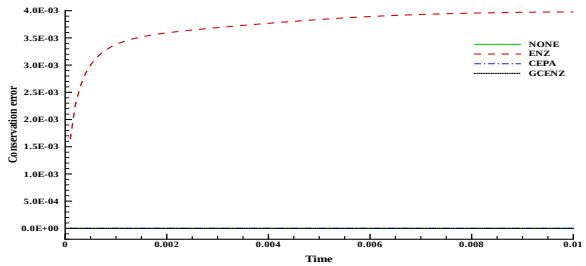

Figure 4: The discrete conservation errors e_{dcon} on Kershaw mesh.

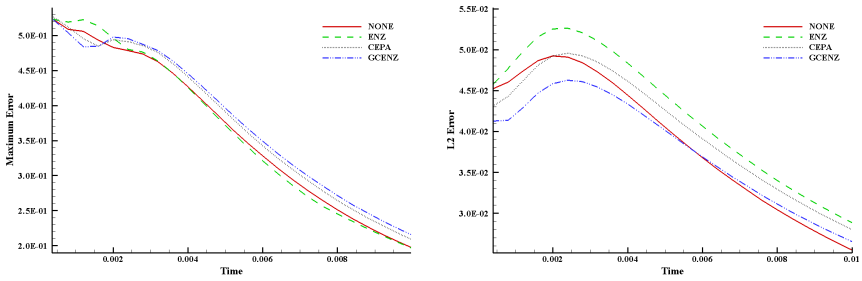

Figure 5: The errors e_{L_∞} and e_{L_2} by NPS, ENZ, CEPA, GCENZ.

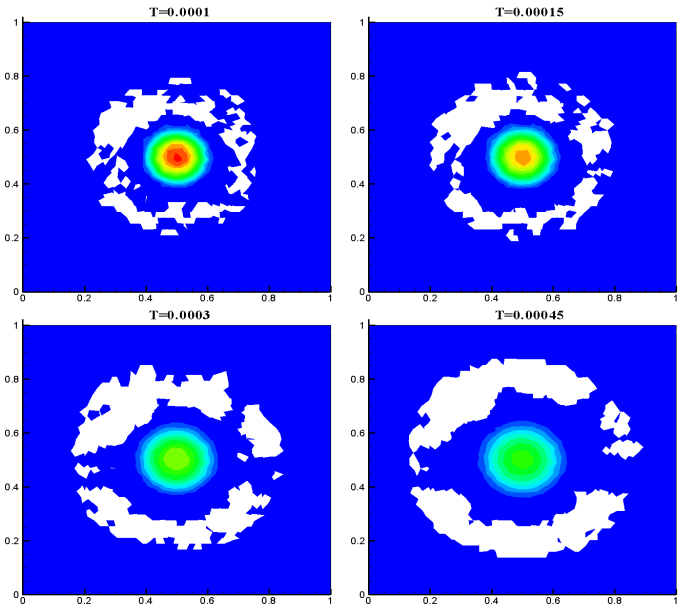

Figure 6: The solutions at $T = 0.0001, 0.00015, 0, 0003, 0.00045$ by the NPS scheme [6] on random triangular mesh.

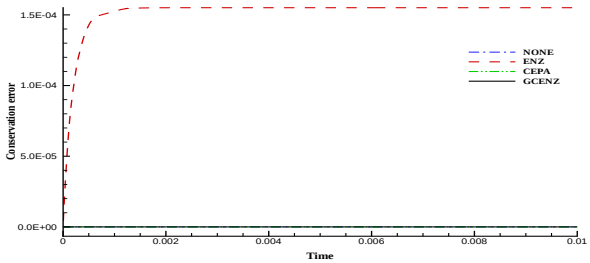

Figure 7: The discrete conservation errors e_{dcon} on random triangular mesh.

formula (38) for three repair methods and the original scheme (7) without using any repair method (denoted as NONE). These three methods are conservative and the conservation errors are unchanged with time. Moreover, the conservation error of CEPA and GCENZ are much smaller than that of ENZ. The GCENZ method is strictly conservative and the conservation error is almost the same as that of the original scheme.

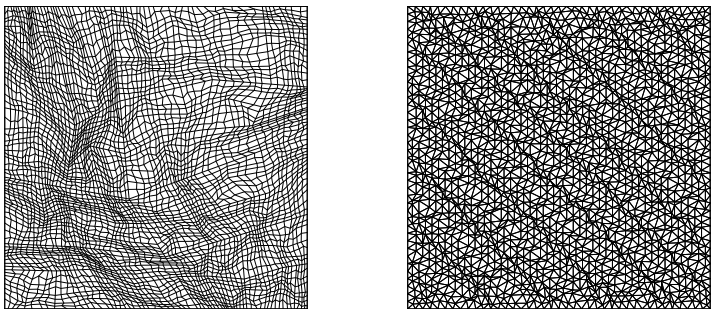

(a) Shestakov mesh (b) Random triangular mesh

Figure 8: The two kinds of computational grids.

Fig. 5 displays the L_∞ and L_2 errors from the scheme (7) and three different repair algorithms. It can be seen that both the L_∞ and L_2 errors using GCENZ and CEPA method are smaller than those of ENZ.

Next, we test this problem on random triangular meshes with the number of cell being 40×40. The numerical solutions on random triangular meshes are shown in Fig. (6)-(7). Fig. 6 shows the numerical solution of the scheme (7) at four different times. The blank part in figures are negative cells and the number of negative cells is decreasing with time. From the Fig. 7, we can conclude that GCENZ preserves the local conservation, and its conservation error is almost the same as that of the original scheme and much smaller than that of ENZ.

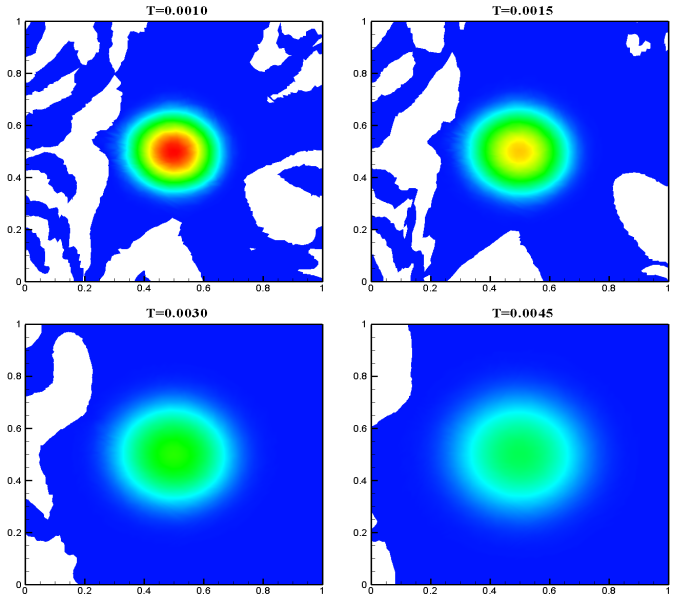

Figure 9: The solutions at $T = 0.001, 0.0015, 0, 003, 0.0045$ by NPS scheme on 64×64 Shestakov mesh.

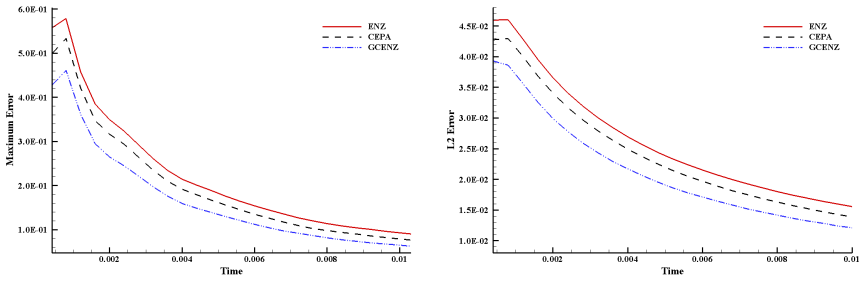

Figure 10: The errors e_{L_∞} and e_{L_2} by ENZ, CEPA, GCENZ on Shestakov mesh.

Example 2 Consider the following nonlinear model with Neumann boundary condition:

(41)
$$\begin{cases} \frac{\partial u}{\partial t} - \mathrm{div}((1+u)\nabla u) = 0, & (x,y,t) \in \Omega \times (0,T], \\ u(x,y,0) = 10\exp\left(\frac{a^2(x-c)^2+b^2(y-c)^2}{a^2(x-c)^2+b^2(y-c)^2-a^2b^2}\right), & a^2(x-c)^2 + b^2(y-c)^2 < a^2b^2, \\ u(x,y,0) = 0, & a^2(x-c)^2 + b^2(y-c)^2 \geq a^2b^2, \\ (1+u)\frac{\partial}{\partial n}u(x,y,t) = 0, & (x,y) \in \partial\Omega, t \in (0,T], \end{cases}$$

It has the same initial and boundary conditions as Example 1 except for the conductive coefficient being $1 + u$.

First, we solve this problem on the 64×64 Shestakov mesh as shown in Fig. 11(a). Note that this model has no source, and no flux crossing the boundary of

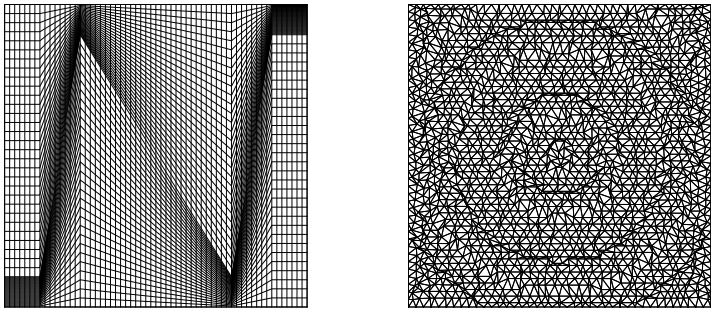

(a) Kershaw mesh (b) Random triangular mesh

Figure 11: Two kinds of computational grids.

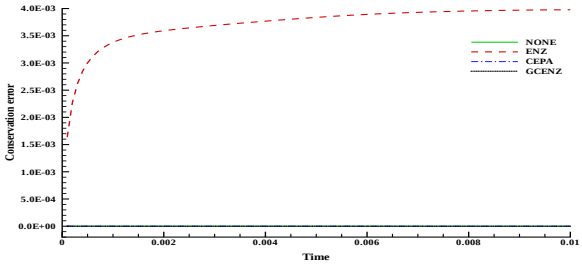

Figure 12: The discrete conservation errors e_{dcon} of different repair methods on Shestakov mesh.

domain, moreover the initial values are nonnegative. The exact solution of (41) is nonnegative due to maximum principle. However, there are many cells with negative values of the numerical solution by the scheme (7) as shown in Fig. 9. The comparison of L_2, L_∞ errors and the conservation error by different repair methods are presented in Figs. 10 and 12.

The errors e_{L_∞} ,e_{L_2} for the ENZ, CEPA and CENZ on the Shastakov grids are compared in Fig. 10. It shows that the errors from the conservative repair methods CEPA and GCENZ are smaller than those from ENZ, thus the GCENZ method is more accurate than CEPA.

The conservation errors of three repair methods and the original scheme are presented in Fig. 12. One can see that the conservation error of the GCENZ is almost the same as that of the scheme (7) and CEPA repair method. In contrast, the conservation errors produced by ENZ method is much larger than that of others.

We also compute this problem on 40×40 random triangular mesh as shown in Fig. 11(b). Fig. 13 shows the plot of the numerical solutions at different time where the blank part represents negative cells. The similar results about conservation are presented in Fig. 14.

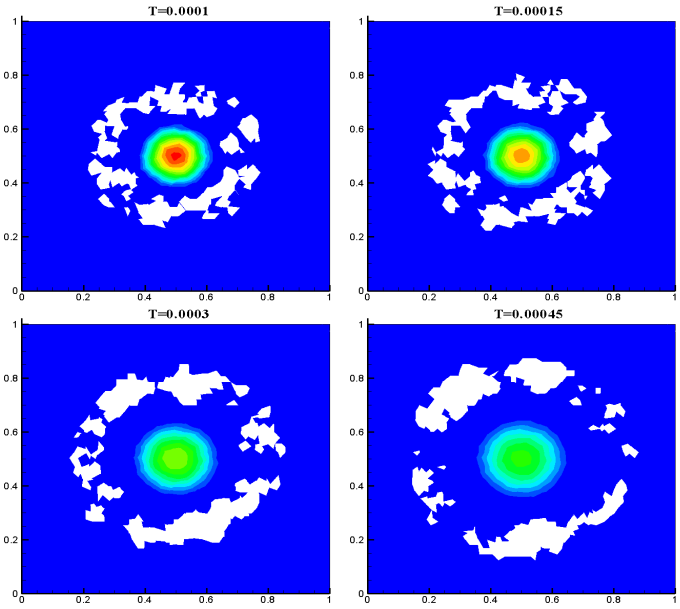

Figure 13: The solutions at $T = 0.001, 0.0015, 0, 003, 0.0045$ by NPS scheme on 40×40 random triangular mesh.

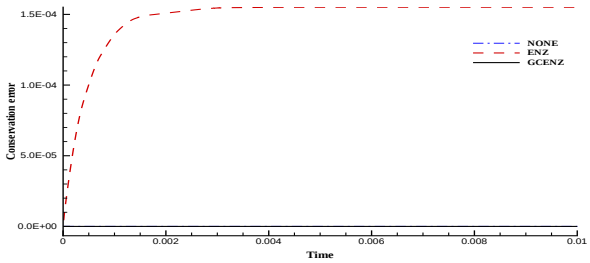

Figure 14: The discrete conservation errors e_{dcon} by different repair methods on random triangular mesh.

5. Conclusions

In this paper, we develop a new conservative enforcing positivity-preserving algorithm (GCENZ) for the finite volume scheme of diffusion equations. It is a posterior repair strategy and can be applied to both structure and unstructured meshes. Three repair algorithms are compared numerically, including (i) the trick of directly setting the negative values to zero (ENZ), which was commonly used in applications, (ii) an existing conservative enforcing positivity-preserving algorithm (CEPA), (iii) and our GCENZ algorithm. The numerical examples show that GCENZ can keep the positivity of solution, and in terms of the conservation it is much better than ENZ, and in terms of L_2 error it is better than ENZ and CEPA, moreover, in terms of L_∞ error it is approximate to ENZ and CEPA.

References

[1] I. Aavatsmark, An introduction to multipoint flux approximations for quadrilateral grids, Comput. Geosci. 6(3-4) (2002) 405-432.
[2] E. Bertolazzi, G. Manzini, A second-order maximum principle preserving volume method for steady convection-diffusion problems, SIAM J. Numer. Anal. 43 (2005) 2172-2199.
[3] A. Draganescu, T. F.Dupont, Lr Scott, Failure of the discrete maximum principle for an elliptic finite element problem, Math. Comput. 74(249) (2005) 1-23.
[4] D. S. Kershaw, Differencing of the diffusion equation in Lagrangian hydrodynamic codes, J. Comput. Phys. 39 (1981) 375-395.
[5] D. Kuzmin, M. J. Shashkov, D. Svyatskiy, A constrained finite element method satisfying the discrete maximum principle for anisotropic diffusion problems, J. Comput. Phys. 228 (2009) 3448-3463.
[6] D. Y. Li, H. S. Shui, M. J. Tang, On the finite difference scheme of two-dimensional parabolic equation in a non-rectangular mesh, J. Numer. Methods Comput. Appl. 1 (1980) 217-224.
[7] K. Lipnikov, M. Shashkov, D. Svyatskiy, The mimetic finite difference discretization of diffusion problem on unstructured polyhedral meshes, J. Comput. Phys. 211(2) (2006) 473-491.
[8] K. Lipnikov, M. Shashkov, I. Yotov, Local flux mimetic finite difference methods, Numer. Math. 112(1) (2009) 115-152.
[9] R. Liska and M. Shashkov, Enforcing the discrete maximum principle for linear finite element solutions of second-order elliptic problems, Commun. Comput. Phys. 3(4) (2008) 852-877.
[10] J. E. Morel, J. E. Deney, Jr M. L. Hall, S. W. White, A cell-centered Lagrangian-Mesh diffusion differencing scheme, J. Comput. Phys. 103 (1992) 286-299.
[11] C. Le Potier, Finite volume monotone scheme for highly anisotropic diffusion operators on unstructured triangular meshes, C. R. Acad. Sci. Paris. Ser.I. 341 (2005) 787-792.
[12] C. Le Potier, A nonlinear finite volume scheme satisfying maximum and minimum principles for diffusion operators, Int. J. Finite Volumes. 6 (2009) 1-20.
[13] Z.M. Gao, J.M. Wu, A linearity-preserving cell-centered scheme for the heterogeneous and anisotropic diffusion equations on general meshes, Int. J. Numer. Meth. Fluids 67 (2011) 2157-2183.
[14] P. Sharma, G. W. Hammett, Preserving monotonicity in anisotropic diffusion, J. Comput. Phys. 227 (2007) 123-142.
[15] Z.Q. Sheng, G.W. Yuan, A nine point scheme for the approximation of diffusion operators on distorted quadrilateral meshes, SIAM J. Sci. Comput. 30 (2008) 1341-1361.
[16] Z. Q. Sheng , J. Y. Yue , G. W. Yuan, Monotone finite volume schemes of nonequilibrium radiation diffusion equations on distorted meshes, SIAM J. Sci. Comput. 31 (2009) 2915-2934.
[17] S. Wang, G. W. Yuan, Y. H. Li, Z. Q. Sheng, Discrete maximum principle based on repair technique for diamond type scheme of diffusion problems, Int. J. Numer. Meth. Fluids 70 (2012) 1188-1205.
[18] J.M. Wu, Z.H. Dai, Z.M. Gao, G.W. Yuan, Linearity preserving nine-point schemes for diffusion equation on distorted quadrilateral meshes, J. Comput. Phys. 229 (2010) 3382-3401.
[19] J.M. Wu, Z.M. Gao, A nine-point scheme with explicit weights for diffusion equations on distorted meshes, Appl. Numer. Math. 61 (2011) 844-867.
[20] Y. Z. Yao, G. W. Yuan, Enforcing positivity with conservation for nine-point scheme of nonlinear diffusion equations, Comput. Methods Appl. Mech. Engrg. 223-224 (2012) 161-172.
[21] G. W. Yuan, Z. Q. Sheng, J. Y. Yue, The finite volume scheme preserving the positivity for diffusion equation, Sci. China Math. 42(8) (2012) 1-21.
[22] G. W. Yuan , Z. Q. Sheng , Monotone finite volume schemes for diffusion equations on polygonal meshes, J. Comput. Phys. 227 (2008) 6288-6312.

School of Mathematical science, University of Science and Technology of China, Hefei 01130, Anhui, P. R. China;, National Key Laboratory of Science and Technology on Computational Physics, Institute of Applied Physics and Computational Mathematics, P. O. Box 8009, Beijing 100088, P. R. China;, School of Mathematics, Physics and Biological Engineering, Inner Mongolia University of Science and Technology, Baotou 014010,Inner Mongolia, P. R. China

E-mail: cfj503@mail.ustc.edu.cn

Laboratory of Computational Physics, Institute of Applied Physics and Computational Mathematics, P. O. Box 8009, Beijing 100088, P. R. China

E-mail: yao_yanzhong@iapcm.ac.cn, yylongustc2003@aliyun.com, yuan_guangwei@iapcm.ac.cn